OPTIMAL TRAJECTORIES FOR LOW ALTITUDE, HIGH ACCELERATION ICBM INTERCEPTION

by

THOMAS WHITNEY EAGLES

B. S., Kansas State University, 1966

A MASTER'S REPORT

submitted in partial fulfillment of the

requirements for the degree

MASTER OF SCIENCE

Department of Mechanical Engineering

KANSAS STATE UNIVERSITY
Manhattan, Kansas

1968

Approved by:

Major Professor

TABLE OF CONTENTS

LIST OF TABLES

LIST OF FIGURES

CHAPTER I

THE PROBLEM

Introduction

In recent months, the United States has decided to deploy an anti-ballistic missile system. This system employs two missiles, one for high altitude, long range interception (the Spartan) and the other for low altitude, short range interception (the Sprint). The mission of the Sprint is to provide "insurance", i.e., to get the targets that Spartan missed. Sprint will intercept targets at altitudes of 100,000 feet or less, and will have an acceleration capability of over 100g (11).*[1]

The difficulty of the missile interception problem is primarily due to the short time available for interception. An ICBM warhead just entering the atmosphere is traveling at nearly 18,000 miles per hour. Thus, every second of flight brings it five miles closer to the target. The defending radar system has very little time in which to detect the warhead and define its trajectory --- less than three minutes, according to one source (10).* It is advantageous to fire the interceptor as late as possible, in order to give the radar maximum time to track the target and thus to refine the trajectory calculations. The only optimum trajectory for the interceptor is a minimum-time trajectory, because this will allow the interceptor to be fired as late as possible (9).*

---

[1]Numbers in starred parentheses stand for the numbered references at the end of this report.

From another point of view, it should be noted that, for a constant-thrust interceptor, minimum time implies minimum fuel consumption, so the interception could be made at the largest possible distance from the launch point.

With the foregoing facts in mind, the purpose of this report was twofold:

1) To derive the necessary conditions for a minimum-time trajectory to a fixed point in range-altitude space,

and

2) to numerically integrate the equations derived in part one for a hypothetical "Sprint-class" interceptor and use the results in a realistic scheme for interception.

Physical Assumptions

A picture of the missile in flight, along with the forces acting on it, is presented in Figure 1, and Table 1 is a list of nomenclature. The assumptions made in this development were :

1) Planar motion

2) No lift ; thus the only way to control the flight path is by thrust vectoring

3) Constant thrust

4) Flat earth, constant g

5) Drag is a function of altitude and velocity, i.e., $D = D(h,V)$

6) Mass is a linear function of time, i.e., $m = m_0 - m't$.[1]

The problem is to find the time histories of the problem variables x, h, V, A, and B such that the time of flight between (x_i, h_i) and (x_f, h_f) is a minimum.

---

[1] Prime superscripts denote differentiation with respect to time.

TABLE I

Nomenclature

T . . . . Thrust magnitude, lbf.

D . . . . Drag magnitude, lbf.

g . . . . Acceleration of gravity, 32.174 ft/sec^2

m . . . . Mass of interceptor, slugs

f subscript . . . . Final value

i subscript . . . . Initial value

"Problem Variables".

x . . . . Range, feet

h . . . . Altitude, feet

V . . . . Velocity magnitude, ft./sec.

A . . . . Angle between velocity vector and horizontal, measured from horizontal, positive counterclockwise.

B . . . . Angle between thrust vector and velocity vector, measured from velocity vector, positive counterclockwise ; also called "control variable" and "thrust angle"

"L Variables":

L_1 . . . . Lagrange Multiplier associated with x

L_2 . . . . "   "   "   " h

L_3 . . . . "   "   "   " V

L_4 . . . . "   "   "   " A

CHAPTER II

NECESSARY CONDITIONS FOR A MINIMUM-TIME TRAJECTORY

The problem of finding a minimum-time trajectory between two points in range-altitude space resembles the classical Brachistochrone problem of the Calculus of Variations (1)[*], and a similar indirect method was used in this report. Specifically, the problem was formulated as a Mayer problem in the Calculus of Variations. A short outline of the Mayer problem as a special case of the Bolza problem is given in Appendix 1.

Equations of Motion

From Figure 1, a force balance on the missile provides the following equations:

$$mV' = TcosB - mgsinA - D \tag{1}$$

$$mVA' = TsinB - mgcosA \tag{2}$$

The kinematic relationships are

$$x' = VcosA \tag{3}$$

$$h' = VsinA \tag{4}$$

Formulation of the Variational Problem

There are many ways to formulate a problem to minimize time. First of all, an expression for the time of flight must be found. Any one of equations (1) to (4)

could be solved for dt and an expression for the time of flight, formed. From (1),

$$t_f - t_i = \int_{V_i}^{V_f} (m/(T\cos B - mg\sin A - D))\,dV \; ;$$

from (2),

$$t_f - t_i = \int_{A_i}^{A_f} (mV/(T\sin B - mg\cos A))\,dA \; ;$$

from (3),

$$t_f - t_i = \int_{x_i}^{x_f} (1/V\cos A)\,dx \; ;$$

from (4)

$$t_f - t_i = \int_{h_i}^{h_f} (1/V\sin A)\,dh.$$

Any of these formulations gives rise to a Lagrange problem, that is, the extremization of an integral subject to side constraints. However, since the problem at hand is in range-altitude space, it would seem wise to choose an expression with x or h as the independent variable as in the last two. At least one author has formulated the problem in this manner (7).[*]

All of the foregoing methods effectively eliminate time from the calculations, leaving velocity, range altitude, or path angle as the independent variable. A much simpler formulation is that of Mayer, in which case time is the independent variable ; by this method of formulation, a more general class of problems can be treated with the same equations (3).[*]

Mayer Problem

The Mayer problem is a special case of the problem of Bolza, and both are outlined in Appendix 1. Applying the Mayer formulation to the present problem, we must first rearrange Equations (1) through (4) and introduce the new functions, P_i :

$$P_1 = x' - V\cos A = 0, \tag{5}$$

$$P_2 = h' - V\sin A = 0, \tag{6}$$

$$P_3 = mV' - T\cos B + mg\sin A + D = 0, \tag{7}$$

and

$$P_4 = mVA' - T\sin B + mg\cos A = 0. \tag{8}$$

The augmented function, F, is defined as

$$F = L_1P_1 + L_2P_2 + L_3P_3 + L_4P_4 \tag{9}$$

where the L's are, in general, functions of t.

Euler-Lagrange Equations

The Euler-Lagrange equations for this problem are :

$$L_1' = 0, \tag{10}$$

$$L_3D_h - L_2' = 0, \tag{11}$$

$$L_1\cos A + L_2\sin A - L_3(D_V - m') - L_4mA' + L_3'm = 0, \tag{12}$$

$$L_1V\sin A - L_2V\cos A + L_3mg\cos A - L_4(mg\sin A + mV' + m'V) = 0, \tag{13}$$

and

$$L_3T\sin B - L_4T\cos B = 0. \tag{14}$$

Since Equation (14) is algebraic, it enables us to eliminate one of the L's, specifically L_4:

$$L_4 = L_3 \tan B. \tag{15}$$

Upon substituting (15) into (12) and (13), rearranging the equations, including Equations (5) through (8), and noting that Equation (10) merely says that $L_1 =$ constant, we arrive at a set of seven first-order ordinary differential equations in the seven unknowns $x, h, V, A, B, L_2,$ and L_3:

$$x' = V \cos A, \tag{16}$$

$$h' = V \sin A, \tag{17}$$

$$V' = 1/m (T \cos B - mg \sin A - D), \tag{18}$$

$$A' = 1/mV (T \sin B - mg \cos A), \tag{19}$$

$$L_2' = L_3 D_h, \tag{20}$$

$$L_3' = 1/m (L_3 (D_v + mA' \tan B - m') - L_1 \cos A - L_2 \sin A), \tag{21}$$

and

$$B' = (\cos^2 B / mVL_3)(L_1 V \sin A - L_2 V \cos A + L_3 (mg \cos A - mg \sin A \tan B - mV' \tan B - m' V \tan B) - mV L_3' \tan B). \tag{22}$$

This set of equations appears to be of the seventh order in the aggregate, and one would normally expect to need seven boundary conditions. The question which then arises is "how many conditions can be imposed on the problem variables (essential boundary conditions) and how many are natural end conditions involving the L's?" In short, how many physical end conditions can be specified without over-determining the problem? The answer is provided by an analysis due to Kelley (3).

"Effective Order" of a Set of Equations

According to Kelley, in a Mayer problem, the number of boundary conditions which can be imposed on the problem variables is equal to the "effective order" of the set of equations, and this effective order is always one less than the apparent order. This is due to the linearity and homogeneity of the equations in the L variables, and can be seen in the following way. If the initial (or final) values of all three L's are multiplied by the same factor, there is no change in the problem variables. Only the ratios of the L's are significant.

Thus, in the present problem, the effective order of the set of equations is six, so six essential boundary conditions can be imposed on the problem variables.

Boundary Conditions

In this case, the essential boundary conditions chosen were the following:

At $t_i = 0$: $x(0) = 0$, $h(0) = 0$, $V(0) = V_i$, and $A(0) = A_i$. $\qquad$ (23)

At t_f: $x(f) = x_f$ and $h(f) = h_f$. $\qquad$ (24)

The other conditions are natural end conditions, and they are obtained from the transversality condition.

The transversality condition for the present problem is

$$((1 - L_1 V\cos A - L_2 V\sin A - L_3(T\cos B - mg\sin A - D) - L_3\tan B(T\sin B - mg\cos A))\,dt + L_1 dx + L_2 dh + L_3 m\,dV + L_3 mV\tan B\,dA)_i^f = 0.$$

From Equation (23),

$$dx_i = dh_i = dV_i = dA_i = 0.$$

From Equation (24),

$$dx_f = dh_f = 0.$$

Since t_i is fixed at zero,

$$dt_i = 0.$$

Since V_f is open, dV_f is arbitrary ; thus,

$$L_{3f} m_f = 0,$$

and since $m_f \neq 0$,

$$L_{3f} = 0. \tag{25}$$

Note that A_f is open, but $L_{3f} = 0$; therefore, no additional information is gained from this fact.

Since time is to be minimized, t_f cannot be fixed ; therefore, dt_f is arbitrary. Combining this fact with Equation (25), we have

$$(1 - L_1 V \cos A - L_2 V \sin A)_f = 0,$$

or, using Equations (3) and (4),

$$(L_1 x' + L_2 h')_f = 1. \tag{26}$$

This exhausts all possibilities. A total of eight boundary conditions have thus been obtained.

Since L_1 is constant and only ratios of the L's are significant, L_1 can be set equal to 1, and the ratios L_2/L_1 and L_3/L_1 become merely L_2 and L_3 respectively. Also, condition (26) becomes $(x' + L_2 h')_f = 1$.

Chapter III of this report contains a discussion of the application of these boundary conditions.

CHAPTER III

NUMERICAL INTEGRATION OF EULER-LAGRANGE EQUATIONS

The problem as defined in Chapter II involves four initial conditions and four final conditions. If an analytical solution to the set of differential equations could be found, this would pose no problem. However, since no solution could be found, it was necessary to use a numerical integration process, integrating from a specified set of initial conditions and trying to converge on the desired final conditions by varying those initial conditions which were not essential boundary conditions.

In the present problem, the desired final conditions are specified by Equations (24), (25), and (26). The non-essential initial conditions which can be varied to obtain the desired final conditions are B_0, L_{2_0} and L_{3_0}. It is conceivable that, with enough diligence and experience, one could converge on the four specified final values at once, but this possibility was considered to be nil under present circumstances. At this point, then, it was thought advisable to employ a device used by Vincent (8) and called a "flooding technique".

Flooding Technique

This technique is essentially the following :

1) The essential boundary conditions at the initial point are imposed ;

2) arbitrary initial values of B, L_2 and L_3 are imposed ;

3) the equations are integrated to missile burnout ;

4) a check is made to see if the <u>natural</u> end conditions are met (no check is

made on x_f and h_f);

5) the initial values of B, L_2 and L_3 are varied in a systematic fashion, and the process is repeated until the natural end conditions are met; x_f and h_f are allowed to fall where they may ; in this way, optimal trajectories to a field of endpoints may be found.

It is important to note that this process is carried out for a given set of essential initial conditions --- that is, for given values of x_i, h_i, V_i and A_i. The endpoints of the optimal trajectories found by this process form a "locus of optimal endpoints". By changing one or more of the essential initial conditions and performing the flooding process again, a different locus of optimal endpoints may be found. In the present investigation, the initial values of x, h, and V were left at a fixed value throughout ; only A_i was varied over a range of values, a locus of optimal endpoints being obtained for each value of A_i.

Although these trajectories are planar, the concept is easily extended to three-dimensional space by simply rotating each locus around the H-axis. A "surface of optimal endpoints" is thus generated which forms an "umbrella" over the launch site. As noted in Chapter II, this umbrella represents the locus of points farthest from the launch site at which interception can occur.

Model Interceptor

Before numerical results can be obtained, some data on the interceptor must be given. The information released so far (10, 11) regarding the Sprint missile gives only diameter (4.5 feet) , length (27 feet) , acceleration capability (over 100 g) ,

and interception ceiling (under 100,000 feet). Therefore, a typical "Sprint-type" missile fitting at least these meager specifications was proposed in this report. Its characteristics are given in Table 2. The missile was assumed to be fired, like the Sprint, from a launcher, by an explosive process, with a fixed initial velocity of 500 feet per second. This launcher is assumed to be of such design that it allows the missile to be launched with an initial flight path angle (A_i) of anywhere from 30 degrees to 90 degrees.

Information regarding the atmospheric density profile and drag function used in this report is given in Appendix 2. The Runge-Kutta-Gill integration scheme is discussed in Appendix 3.

Numerical Results.

As was noted previously, the initial conditions B_i, L_{2i} and L_{3i} were to be varied in an attempt to converge upon the final values $L_{3f} = 0$ and $x'_f + L_{2f}h'_f = 1$. The left-hand side of the latter equation was set equal to a quantity called PARAM, and the goal was then to obtain the conditions $PARAM_f = 1$ and $L_{3f} = 0$ simultaneously.

In order to get some idea of the influence of changes in B_i, L_{2i} and L_{3i} on $PARAM_f$ and L_{3f}, parametric studies were conducted[2]. In each study, the initial value of one of the variables was changed while the initial value of the others remained fixed. This was done for values of A_i of 30, 60, and 90 degrees. The results of these studies are shown in Figures 2 to 6.

From these graphs, a number of conclusions were drawn. From Figure 6

TABLE 2

SPECIFICATIONS OF MODEL INTERCEPTOR

Number of stages 1

Launch mass . . . . 850 slugs (27,400 lbm.)

Burnout mass . . . . 100 slugs (3,220 lbm.)

Propellant Burning rate . . . . 50 slugs/sec.

Exhaust velocity . . . . 10,000 fps.

Thrust . . . . 500,000 lbf. (constant)

Burning time . . . . 15 seconds

Thrust acceleration . . . . From 26 to 156 g

Frontal area . . . . 20 square feet

it was seen that B_i has very little influence on $PARAM_f$ and L_{3f}. It was found, however, that B_i strongly influenced the values of x_f and h_f. Thus, the following procedure was adopted :

1) Set $B_i = 0$ and converge on the natural end conditions by varying L_{2i} and L_{3i} only ;

2) once the final conditions have been met, vary B_i to obtain a "fan" of near-optimal trajectories (in the sense that $PARAM_f$ and L_{3f} are almost at their required values) to a field of x-h endpoints ;

3) again vary L_{2i} and L_{3i} very slightly to correct the slight errors in $PARAM_f$ and L_{3f} induced by the changing B_i.

This was done for A_i equal to 30, 40, 50, 60, 70, 80, and 90 degrees, and the resulting "fans" of trajectories are shown in Figures 7 to 13. B_i was varied over a range of only ± 10 degrees, because it was felt that anything over these bounds was unrealistic from a physical standpoint.

For each trajectory in Figures 7 to 13, the desired natural end conditions were satisfied as nearly as was possible with the limited time and experience at hand. In all cases, the value of $PARAM_f$ fell within the limits of ± 10. This was found to be adequate due to the non-sensitivity of the trajectory parameters to small changes in $PARAM_f$. However, the trajectory parameters were sensitive to small changes in L_{3f}, and difficulty was experienced in approaching the desired value of $L_{3f} = 0$. In all cases, the value of L_{3f} was below 0.09, and in most cases, it was below 0.05. Further efforts to reduce L_{3f} were unsuccessful.

In the remainder of this report, the trajectories in Figures 7 to 13 are called "optimal trajectories" ; however, they are only near-optimal at best, because the

natural end conditions were not precisely satisfied.

It was thought that one reason for this difficulty was that no bounds were placed on the control variable, B. For a more valid physical model, limits should have been imposed upon B, and this would result in a different problem ; this different problem is discussed in Appendix 4.

Loci of Optimal Endpoints

In the present problem, the missile has a fixed burning time of 15 seconds, and all of the optimal trajectories have endpoints with a final time of 15 seconds. These endpoints form a locus of optimal endpoints, or "15 second locus". There is a locus for each value of A_i, and these loci are shown as the dotted curves at the end of each optimal fan in Figures 7 to 13. Only five trajectories were run within each fan, and the loci of optimal endpoints were found merely by drawing a smooth curve through the endpoints of the five trajectories in each fan.

In Figure 14, all of the fans of optimal trajectories shown in Figures 7 to 13 are superimposed on one graph. It can be seen that the loci overlap, and each locus has one point with the greatest slant range from the launch point. This point is called the extreme optimal endpoint (EOP) for that locus. Since each locus has an EOP, an envelope of EOP's is generated, which represents the absolute maximum distance the missile can reach before burnout. This envelope is shown as the dot-dash curve tangent to each locus of optimal endpoints in Figure 14.

Time History of the Control Variable

Figures 7 to 13 present a helpful physical picture of the optimal trajectories, but the desired quantity is the time history of the control variable, B. These histories are presented in Figures 15 to 21 ; they represent the thrust angle-time relationships which would result in the optimum trajectories shown in Figures 7 to 13.

Comparison Trajectories

In the previous paragraphs, the trajectories obtained were referred to as "optimal" --- that is, minimum-time paths. However, it must be remembered that the conditions used in deriving the trajectory equations were only necessary and not sufficient conditions for a minimum. Therefore, it would be instructive to compare these trajectories with some arbitrary trajectories to the same points. Due to the difficulty of trying to find arbitrary trajectories which pass through given endpoints, this comparison is very hard to make in a numerical study.

This difficulty can be circumvented in the following way : each locus of optimal endpoints represents a 15-second constant-time curve. If any arbitrary trajectory passed through the locus and had an endpoint which fell outside the locus, then it must have crossed the locus at some time earlier than 15 seconds, and, therefore, the "optimal" trajectory to the point which it crossed is not optimal at all. Thus, if the trajectories found in the present study are indeed optimal, then all arbitrary trajectories with the same essential initial conditions should have endpoints which lie on or within the locus of optimal endpoints corresponding to those initial condi-

tions.

The only comparison trajectories used in this study were gravity turn trajectories (defined as trajectories with B $\leqq 0$). For a valid comparison, the optimal and comparison trajectories must have the same essential initial conditions --- in this case, the same x_i, h_i, V_i and A_i. Gravity turns for $A_i = 30$, 40, 50, 60, 70, 80 and 90 degrees, respectively, are shown as the dot-dash curves in Figures 7 to 13. Within the limits of accuracy used in the calculations, the endpoint of each gravity turn fell on the locus of optimal endpoints in each case.[1] In other words, the gravity turns gave the same performance as the optimal trajectories.

In the next section, an interception scheme is presented using the concept of an envelope of EOP's ; since gravity turns were found to yield the same performance, the same argument holds if the locus of gravity turn endpoints is used in place of the envelope of EOP's.

Interception Scheme

Once the envelope of EOP's has been found, it can be rotated about the h-axis to form an "umbrella of EOP's" over the launch site. The coordinates of each point on the umbrella correspond to a unique set of initial conditions. The time of arrival of the interceptor at any point if fired "now" is a known quantity. When an enemy warhead is detected, its future path can be determined, and the point (in space and time) at which it crosses the umbrella can be found. When the time of crossing and the

---

[1]For the case of $A_i = 30$ degrees, the gravity turn did not pass through the locus of optimal endpoints ; thus no direct comparison could be made.

time of arrival match, the interceptor is fired with the initial conditions unique to that point.

Conclusions

It has been shown that, within the limits of accuracy of the calculations, arbitrary trajectories yielded the same performance as the optimal trajectories in the present problem. This was thought to be due to the fact that the natural end conditions for the variational problem could not be satisfied precisely and that the trajectories were, therefore, not true optimums. Another factor was the extremely high thrust and correspondingly high acceleration, which produced nearly straight-line trajectories, whether "optimum" or arbitrary.

Using the flooding technique, an "umbrella" of extreme optimal endpoints has been determined over the launch site, with each point on the umbrella corresponding to a unique set of initial conditions. An apparently feasible interception scheme using this concept has been proposed.
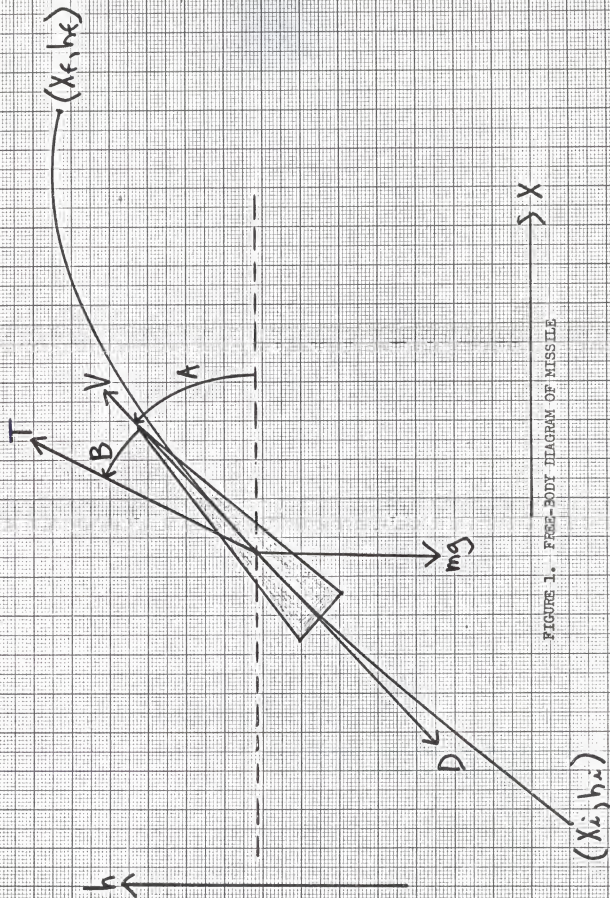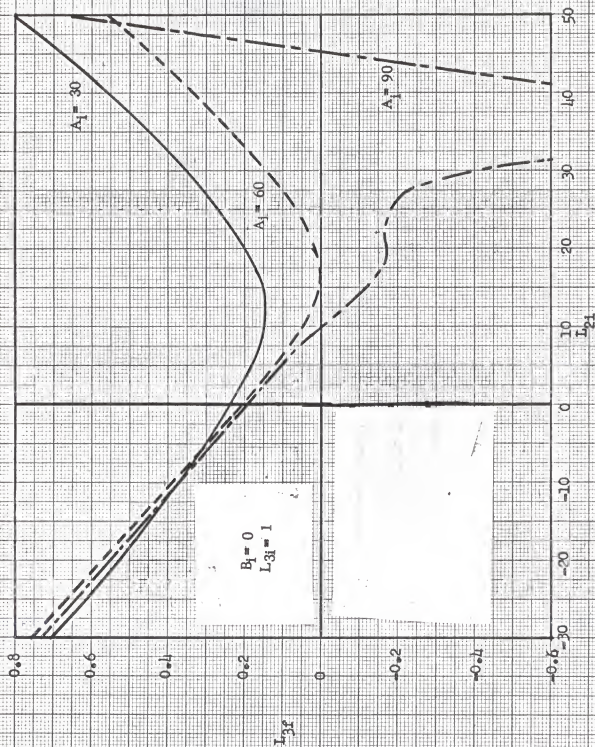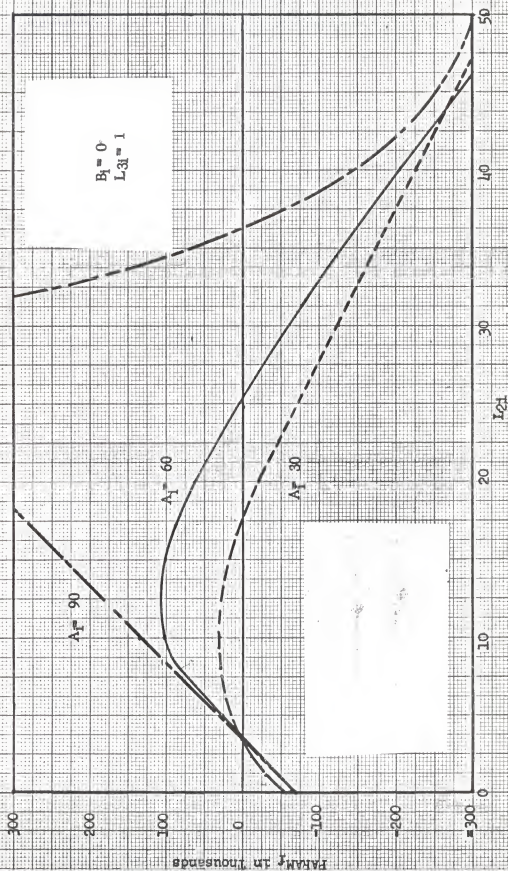
FIGURE 1. FREE-BODY DIAGRAM OF MISSILE

FIGURE 2. L_{3f} vs. L_{21}

FIGURE 3. PARAM$_f$ vs. L$_{21}$

$B_1 = 0$

$L_{21} = 1$

$30^\circ \leq A_1 \leq 90^\circ$

FIGURE 4. L_{1f} vs. L_{3i}

Figure 5. PARAM$_f$ vs. L$_{3i}$

$B_1 = 0$

$L_{21} = 1$

$30^\circ \leq A_1 \leq 90^\circ$

PARAM$_f$ in Thousands
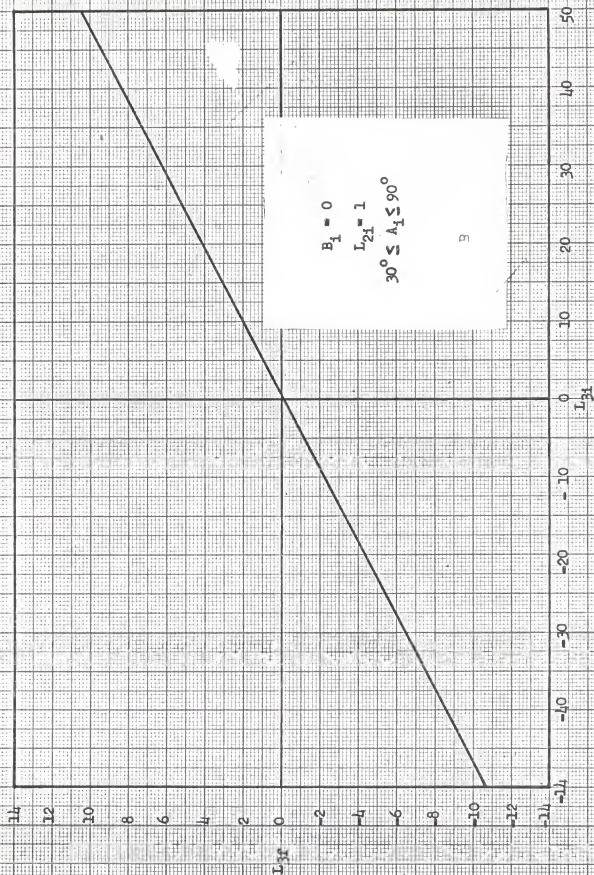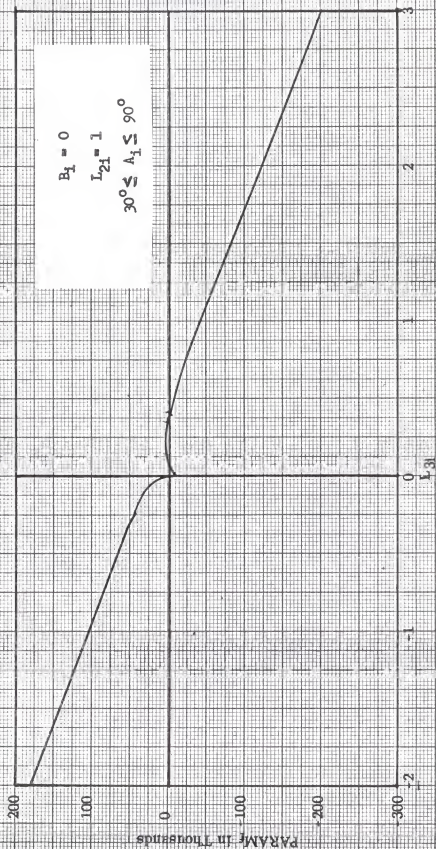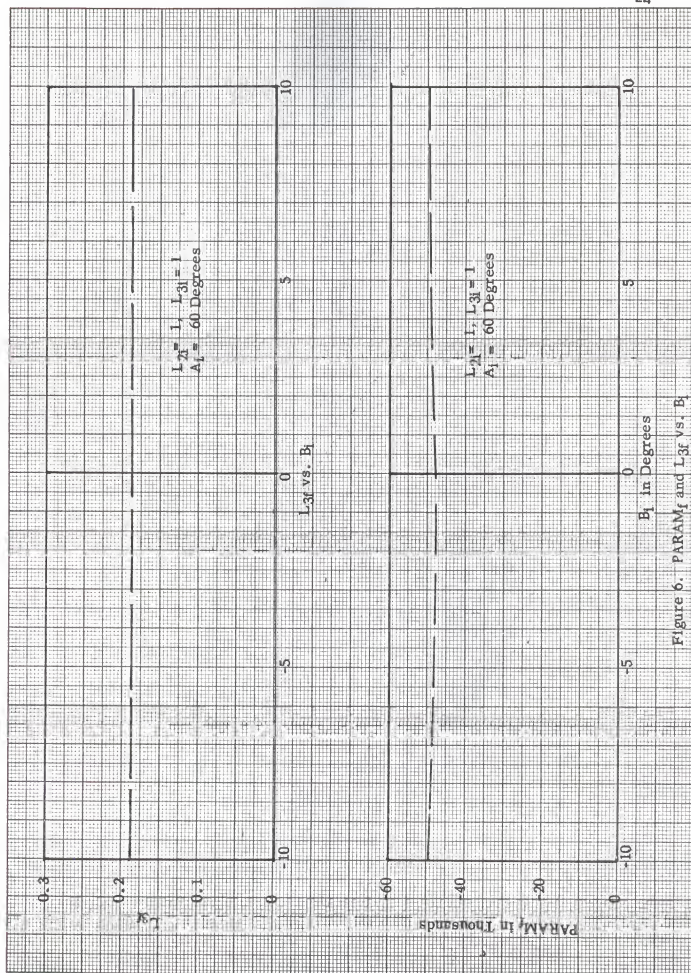
Figure 6. $PARAM_f$ and L_{3f} vs. B_f

$L_{2f} = 1$, $L_{3f} = 1$
$A_f = 60$ Degrees

L_{3f} vs. B_f

$L_{2f} = 1$, $L_{3f} = 1$
$A_f = 60$ Degrees

B_f, in Degrees

L_{3f}

$PARAM_f$, in Thousands
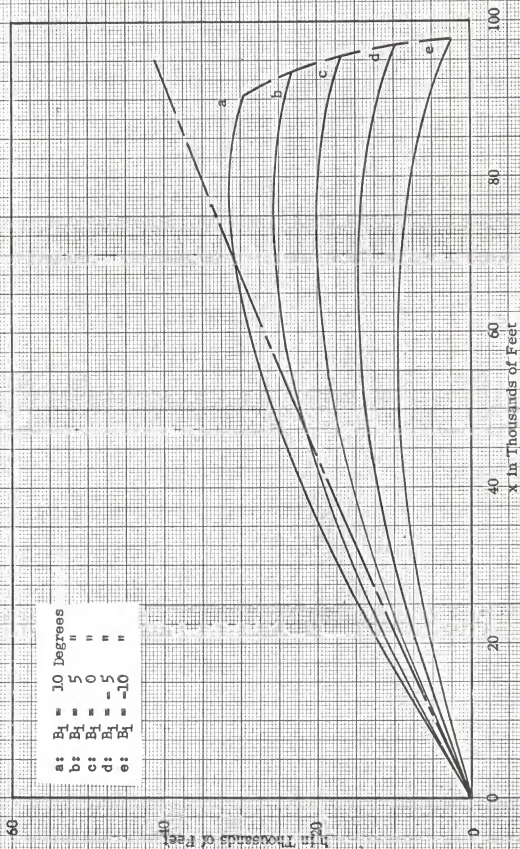
Figure 7. Optimal Trajectories for $A_1 = 30$ Degrees

x in Thousands of Feet

y in Thousands of Feet

		1.0 Degrees
a:	B_1	=
b:	B_1	= 5
c:	B_1	= 0
d:	B_1	= −5
e:	B_1	= −10
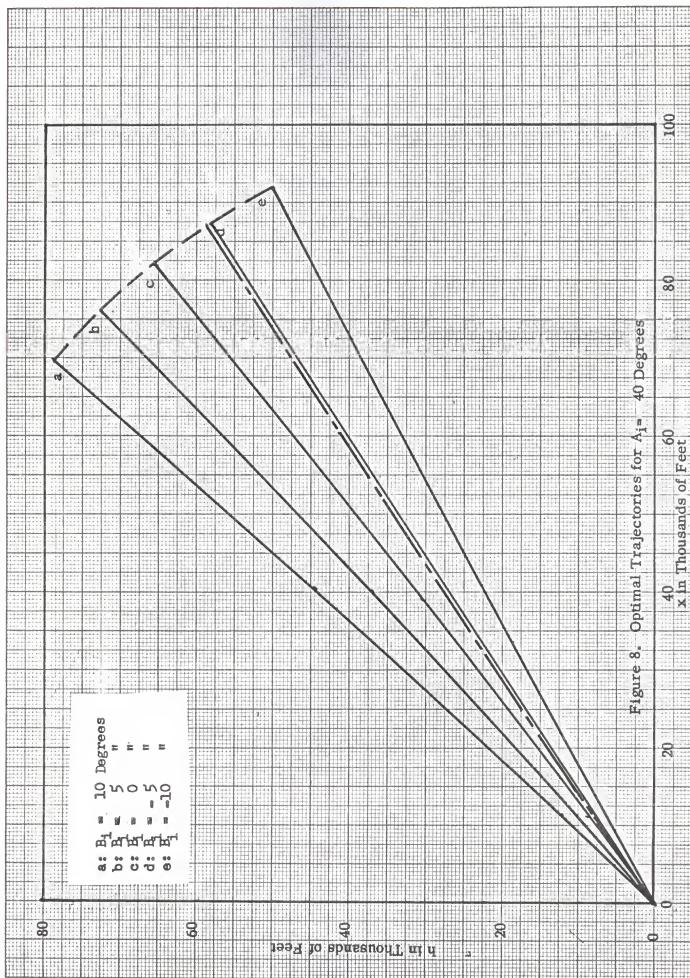
Figure 8. Optimal Trajectories for $A_1 = 40$ Degrees

x in Thousands of Feet

h in Thousands of Feet

	B_1	=	10 Degrees
a:	B_1	=	10 Degrees
b:	B_1	=	5 "
c:	B_1	=	0 "
d:	B_1	=	-5 "
e:	B_1	=	-10 "

a: B_1 = 10 Degrees
b: B_1 = 5 "
c: B_1 = 0 "
d: B_1 = - 5 "
e: B_1 = -10 "
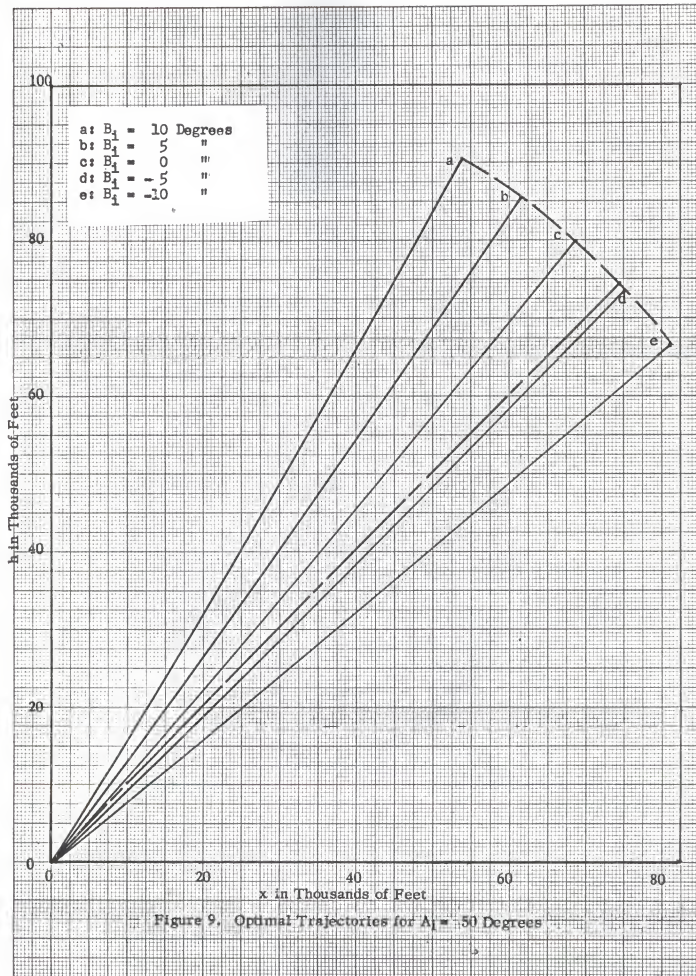
Figure 9. Optimal Trajectories for A_1 = 50 Degrees

h in Thousands of Feet

x in Thousands of Feet
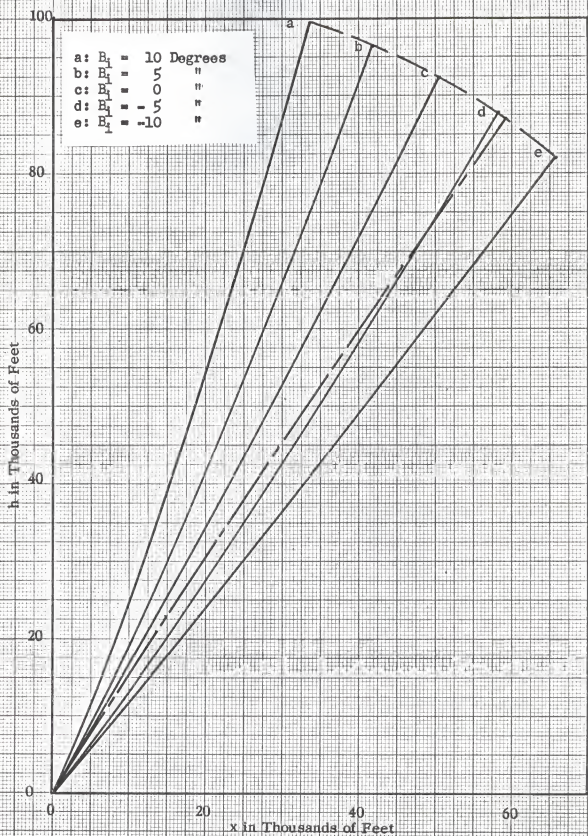
Figure 10. Optimal Trajectories for $A_1 = 60$ Degrees

a: $B_1 = 10$ Degrees
b: $B_1 = 5$ "
c: $B_1 = 0$ "
d: $B_1 = -5$ "
e: $B_1 = -10$ "

h in Thousands of Feet

x in Thousands of Feet

a: $B_1 = 10$ Degrees
b: $B_1 = 5$ "
c: $B_1 = 0$ "
d: $B_1 = -5$ "
e: $B_1 = -10$ "

Figure 11. Optimal Trajectories for $A_1 = -70$ Degrees

h in Thousands of Feet

x in Thousands of Feet

a: $B_1 = 10$ Degrees
b: $B_1 = 5$ "
c: $B_1 = 0$ "
d: $B_1 = -5$ "
e: $B_1 = -10$ "

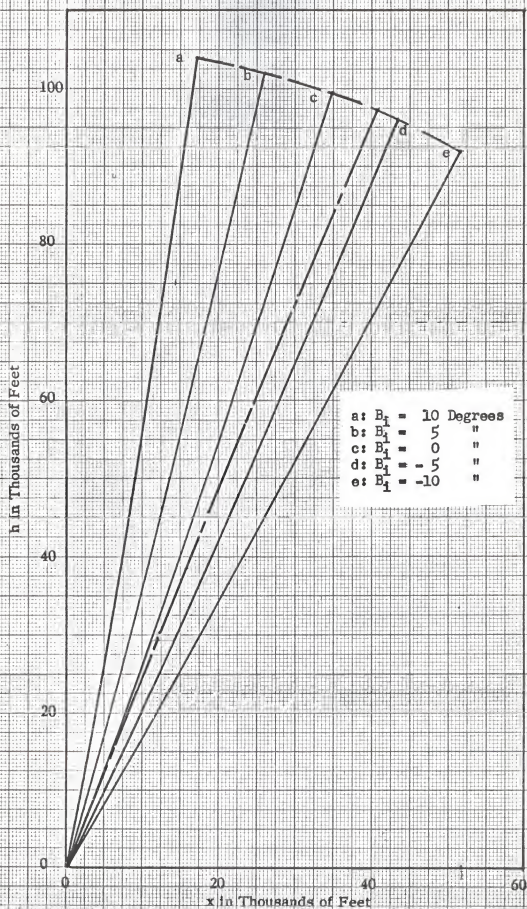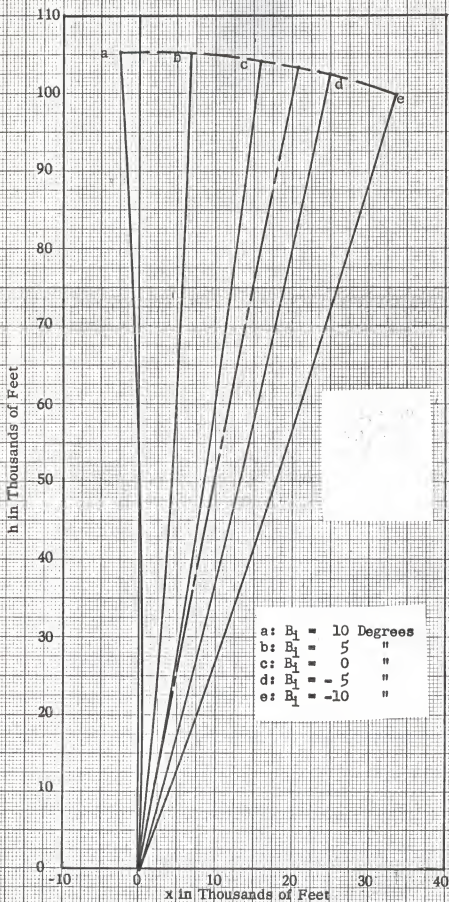Figure 12. Optimal Trajectories for $A_1 = 80$ Degrees
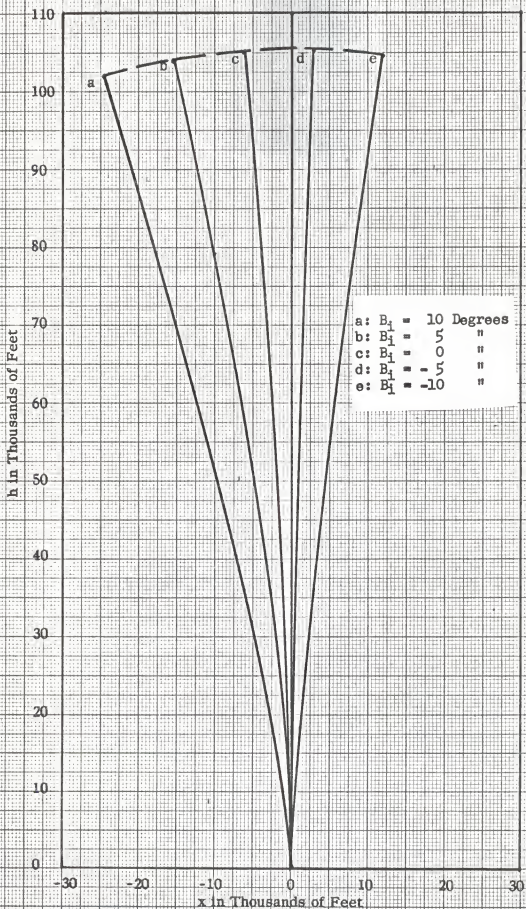
Figure 13. Optimal Trajectories for $A_i = 90$ Degrees

a: $B_i = 10$ Degrees
b: $B_i = 5$ "
c: $B_i = 0$ "
d: $B_i = -5$ "
e: $B_i = -10$ "

h in Thousands of Feet

x in Thousands of Feet

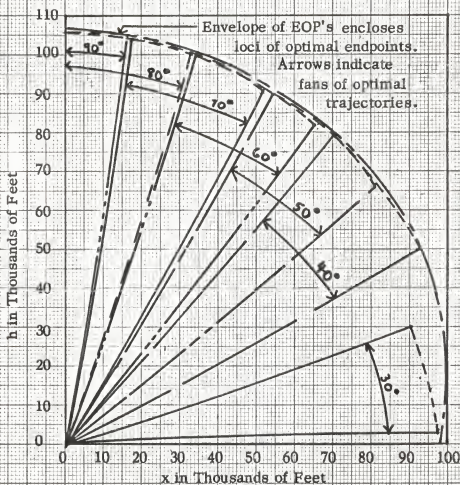Figure 14. Envelope of EOP's

Figure 15. B vs. Time for A$_1$ = 30 Degrees

Figure 16. B vs. Time for A_1 = 40 Degrees

Figure 17. B vs. Time for $A_I = 50$ Degrees

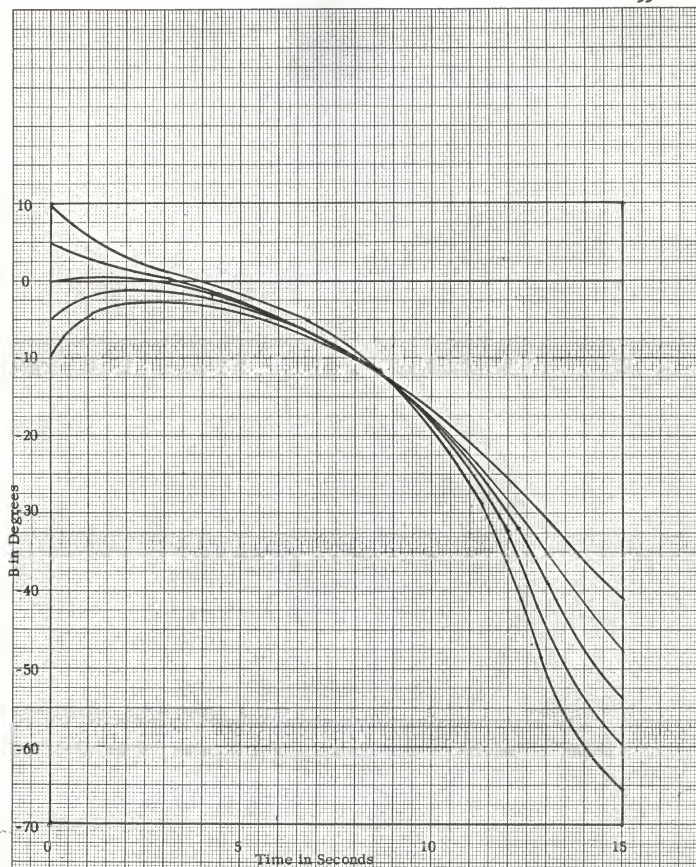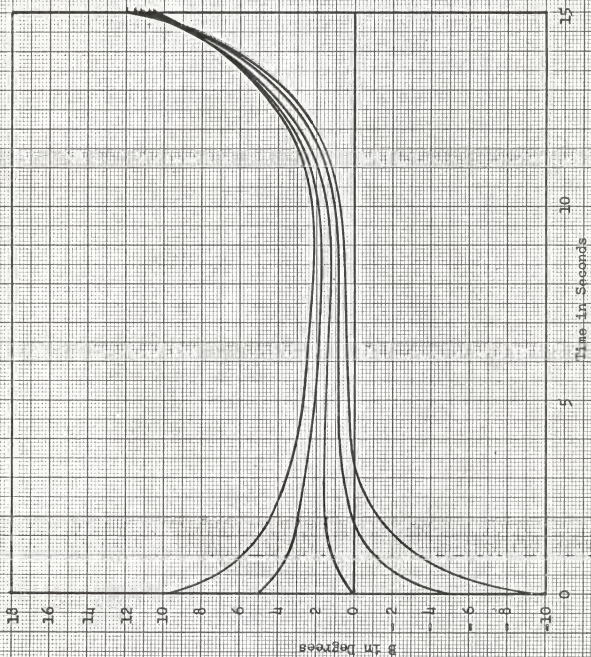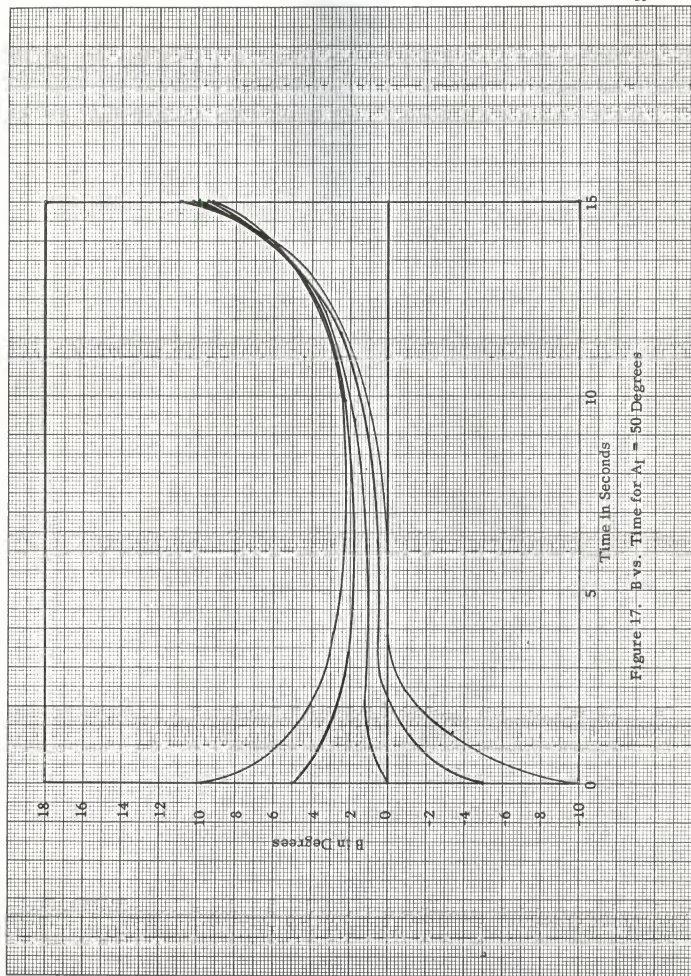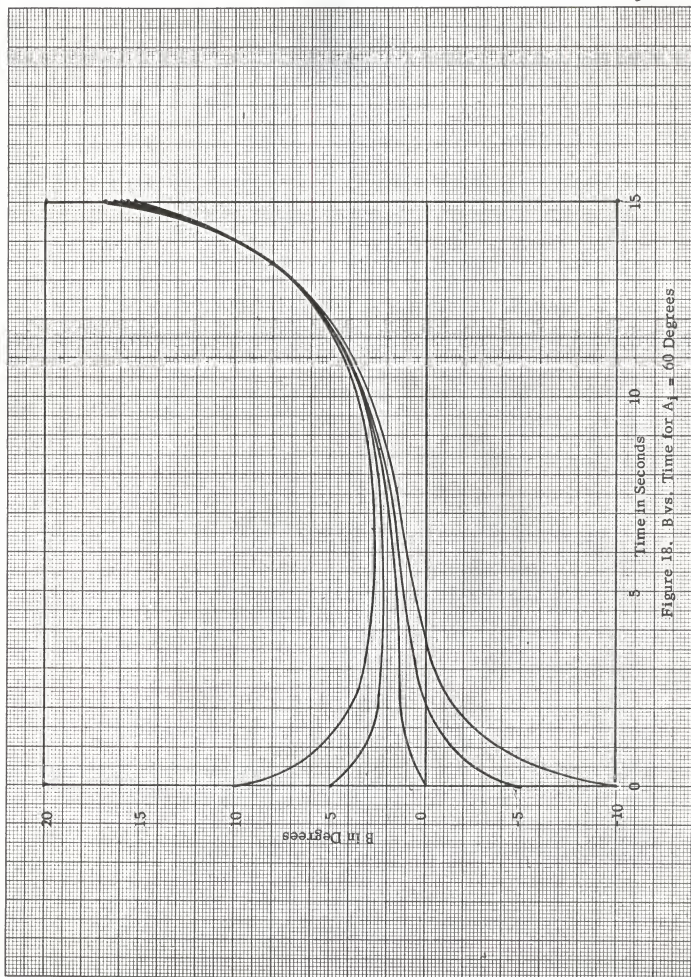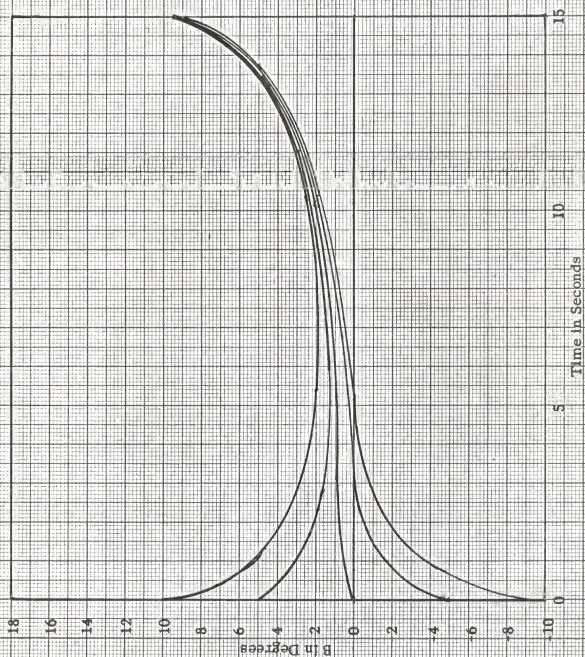Figure 18. B vs. Time for A_1 = 60 Degrees

Time in Seconds
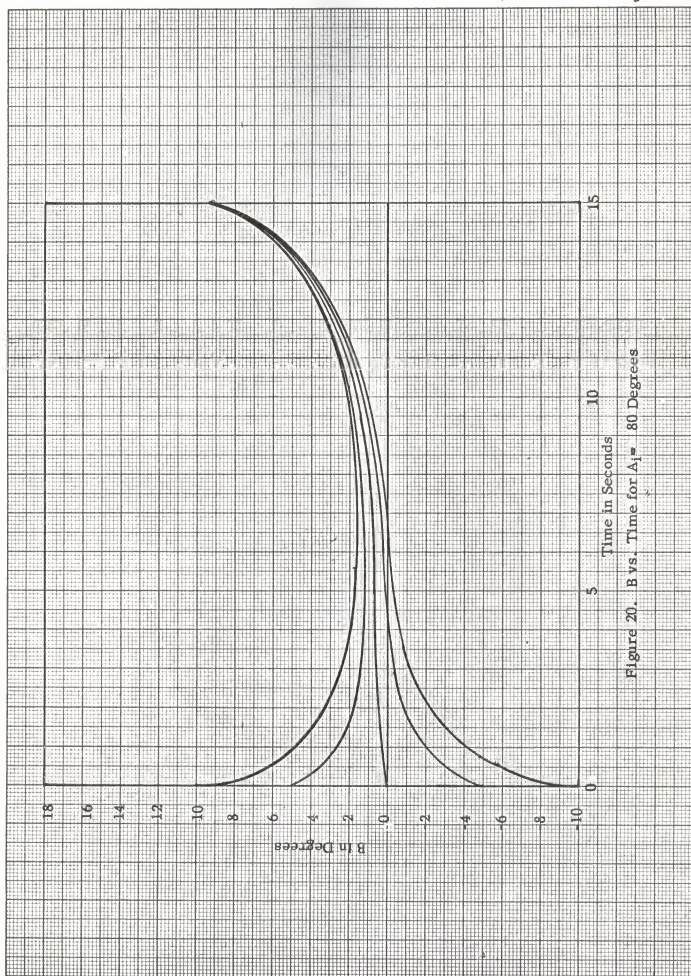
B in Degrees

Figure 19. B vs. Time for $A_1 = 70$ Degrees
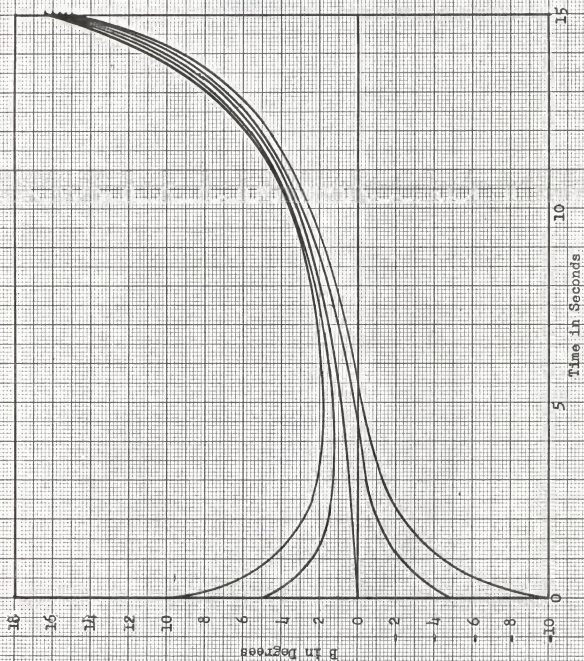
Figure 20. B vs. Time for $A_1 = 80$ Degrees

Figure 21. B vs. Time for $A_1 = 90$ Degrees

LIST OF REFERENCES

1. Akhiezer, N. I., The Calculus of Variations, New York : Blaisdell
    Publishing Company, 1962.

2. Jurovics, Stephen, "Optimum Steering Program for the Entry of a
    Multistage Vehicle Into a Circular Orbit," ARS Journal,
    April 1961 : 518-522.

3. Kelley, Henry J., "An Investigation of Optimal Zoom Climb Techniques,"
    Journal of the Aero/Space Sciences, December 1959 : 794-802.

4. Korn, Granino A. and Korn, Theresa M., "Numerical Calculations and
    Finite Differences," Mathematical Handbook for Scientists and
    Engineers. Second Edition, Chapter 20. New York : McGraw Hill,
    1968.

5. Leitmann, George, Editor, Optimization Techniques with Applications
    to Aerospace Systems, Chapter 4. New York: Academic Press, 1962.

6. Perkins, C.D. and Hage, R.E., Airplane Performance, Stability and
    Control, New York : John Wiley, 1949.

7. Theodorsen, Theodore, "Optimum Path of an Airplane --- Minimum Time
    to Climb," Journal of the Aero/Space Sciences, October 1959 :
    637-642.

8. Vincent, Thomas L. and Brusch, Richard G., Minimum Time Aircraft
    Trajectories Between Two Points in Range Altitude Space, NASA
    CR-631, October, 1966.

9. Willke, Theodore L., "An Asymptotic Method for Guidance of a High-Thrust
    Interceptor," AIAA Student Journal, October 1967, 5 (3) : 119-124.

10. "Anti-Missile Missile," Machine Design, January 1966 : 116-118.

11. "Aerospace Encyclopedia," Aerospace Technology, July 31, 1967 : 67.

APPENDIX 1

THE PROBLEMS OF BOLZA AND MAYER (5)[*]

Bolza Problem

The problem of Bolza in the Calculus of Variations is stated as follows: Given the functional,

$$I = (G(t,y_k))_i^f + \int_{t_i}^{t_f} H(t,y_k,y_k')\,dt \text{ where } k = 1,2,\ldots,n,$$

find the set of functions $y_k(t)$, $k = 1,2,\ldots,n$, which minimizes I while satisfying the constraints

$$P_j(t,y_k,y_k') = 0 \qquad\qquad j = 1,2,\ldots,p(\text{less than } n)$$

and the boundary conditions

$$W_r(t_i,y_{ki}) = 0 \qquad\qquad r = 1,2,\ldots,q$$

and

$$W_r(t_f,y_{kf}) = 0 \qquad\qquad r = q+1,q+2,\ldots,s \text{ (less than } 2n+2).$$

Necessary conditions for the existence of an extremal for I are that the set of y_k's satisfies the Euler-Lagrange equations,

$$d^*F/d^*y_k - d/dt(d^*F/d^*y_k') = 0, \qquad k = 1,2,\ldots,n$$

where

$$F = H + \sum_{j=1}^{p} L_j P_j \ .$$

In the preceding two equations, d^* stands for the symbol for partial differentiation, S stands for the standard summation sign (sigma), and L_j denotes a Lagrange

Multiplier which, in general, is variable with time.

The set of y_k's which extremizes I must also satisfy the p constraint equations, so the differential system to solve consists of n+p equations in the n dependent variables and the p Lagrange Multipliers.

The set of y_k's must also satisfy the transversality condition shown below for all dx, dy_k, dG consistent with the boundary conditions :

$$(dG + (F - \overset{n}{\underset{k=1}{S}}(d^* F/d^* y_k') y_k') dx + \overset{n}{\underset{k=1}{S}}(d^* F/d^* y_k') dy_k) \overset{f}{\underset{i}{}} = 0,$$

where, as before, d^* denotes a partial derivative and S represents the summation sign.

Mayer Problem

The Mayer problem is the special case of the Bolza problem which occurs when H = 0 in the original formulation. For the Mayer problem, all of the foregoing equations hold.

In the present problem, time is the quantity to be minimized, so the function $(G(t, y_k))_i^f$ is merely $t_f - t_i$.

APPENDIX 2

ATMOSPHERIC DENSITY PROFILE AND DRAG FUNCTION(*6)

The atmospheric density profile used in this report was derived by using the basic differential equation for pressure vs. altitude :

$$-dp/p = 1/R \ (dh/T).$$

In this equation p, h, T, and R denote the pressure, altitude, temperature, and gas constant. Plots of temperature vs. altitude were obtained from the NACA Standard Atmosphere, and the above equation was integrated for three altitude ranges --- tropospheric, stratospheric, and above stratospheric. The relation

$$Density = p/gRT$$

was then used to find the density profile. The results were :

h less than 35,000 feet: Density= $.002378(1 - .0000069h)^{4.25}$

h between 35,000 and 70,000 feet: Density = $.000727 \exp \dfrac{35000 - h}{21000}$

h over 70,000 feet: Density = $\dfrac{.000136}{((317 + .00109h)/ 393)^{18.5}}$

The units on density and h are slugs /ft^3 and feet, respectively.

Drag Function

From Reference 6, the drag equation is

$$D = C_D (Rho) V^2 A/2,$$

where Rho, A, and C_D are the atmospheric density, frontal area of the missile, and

the drag coefficient, respectively.

The profile drag coefficient for a streamlined body of revolution was given as 0.05 ; since no lift is present, this is the total drag coefficient. The frontal area of the missile was 20 square feet. Substituting these values into the drag equation, we have

$$D = (Rho)V^2/2,$$

which is the equation used in this study.

APPENDIX 3

RUNGE-KUTTA-GILL NUMERICAL INTEGRATION SCHEME (4)[*]

The Runge-Kutta-Gill (RKG) process is one of many variations of the basic Runge-Kutta method. It is called a "fourth order" method because the formulas for $y_{i, j+1}$ are exact for $f_i = 1$, x, x^2, x^3, and x^4.

Given a set of differential equations

$$y_i' = f_i(y_i, t), \quad i = 1, 2, \ldots, N,$$

the domain of integration is broken up into P intervals ; the size of each interval (step size) is $H = 1/P$. If the values of y_i are known at a particular point in the domain, say point j, these values are denoted by the notation $y_{i, j}$. The values of $y_{i, j+1}$ are then given by the following formulas:

$$y_{i, j+1} = y_{i, j} + 1/6(A_i + 2(1 - (1/2)^{-1})B_i + 2(1 + (1/2)^{-1})C_i + D_i)$$

where

$$A_i = Hf_i(x_j, y_j),$$

$$B_i = Hf_i(x_j + H/2, y_j + A_i/2),$$

$$C_i = Hf_i(x_j + H/2, y_j - (1/2 - (1/2)^{-1})A_i + (1 - (1/2)^{-1})B_i),$$

$$D_i = Hf_i(x_j + H, y_j - (1/2)^{-1}B_i + (1 + (1/2)^{-1})C_i).$$

APPENDIX 4

BOUNDED CONTROL (5)[*]

In this study, the control variable was unbounded. A more realistic assumption would have been that the control variable (thrust angle) has limits --- for example, $\pm$ 10 degrees. In order to account for this, the following constraint equation must be imposed :

$$(B + 10) \ (10 - B) = K^2.$$

K is a new real variable. This is a new holonomic constraint on the problem, and gives rise to another Euler-Lagrange equation involving K and another Lagrange Multiplier L_5. This equation is

$$KL_5 = 0. \tag{A4.1}$$

The Euler-Lagrange equation for B is also changed, becoming

$$L_3 T \sin B - L_4 T \cos B - L_5 2B = 0. \tag{A4.2}$$

The addition of these new equations greatly changes the nature of the problem, primarily by introducing discontinuous solutions for B(t). Due to the limited scope of this study, only continuous solutions with unbounded control were studied.

ACKNOWLEDGEMENTS

I would like to thank several people for their help and inspiration regarding this study.

Dr. James M. Bowyer, my major professor, gave me the benefit of his considerable experience with variational problems; of equal value was the freedom he gave me in allowing me to work on a problem of my own choosing. Dr. Hugh Walker taught me what I know about numerical methods, and provided me with a Runge-Kutta-Gill computer subroutine which he wrote. Dr. J. M. Marr was kind enough to sit on my master's committee on short notice, due to the death of one of the members; Dr. T. B. Swearingen called my attention to reference 8, which was invaluable.

My mother, Mrs. Helen Eagles, typed the manuscript (formulas and all) a feat for which I will be eternally grateful.

Finally, a special note of thanks goes to the late Dr. Ralph Sanger, who first introduced me to the Calculus of Variations.

OPTIMAL TRAJECTORIES FOR LOW ALTITUDE, HIGH
ACCELERATION ICBM INTERCEPTION

by

THOMAS WHITNEY EAGLES

B. S., Kansas State University, 1966

_____

AN ABSTRACT OF A MASTER'S REPORT

submitted in partial fulfillment of the

requirements for the degree

MASTER OF SCIENCE

Department of Mechanical Engineering

KANSAS STATE UNIVERSITY
Manhattan, Kansas

1968

A pproved by:

James M. Bowyer Jr
Major Professor

The anti-ballistic missile system which the United States is now deploying involves two missiles, the Spartan and the Sprint, for high and low altitude targets respectively. This report focuses on the low altitude portion with the following two purposes: to derive the necessary conditions for minimum-time trajectories for a low altitude, high acceleration interceptor such as the Sprint and to integrate numerically the resulting equations so as to find some optimal trajectories for a proposed model interceptor in the Sprint class.

The physical assumptions that the vehicle motion was in a vertical plane, that no lift was present, and that the flight path was determined by the thrust angle alone were made. Mass was assumed to be a linear function of time, drag was considered to be a function of altitude and velocity, and thrust was assumed to be constant. No bounds were placed on the control variable (thrust angle).

The problem was formulated as a Mayer problem in the Calculus of Variations, and the Euler-Lagrange equations and transversality condition were derived. The number of essential boundary conditions allowed was determined, and natural end conditions were found from the transversality condition.

A model interceptor was proposed, and, using data for this model, the Euler-Lagrange equations were integrated numerically to missile burnout. A locus of "extreme optimal endpoints" was determined which represented the locus of points farthest from the launch site at which interception could occur. The concept was extended to three dimensions by rotating this locus around the altitude axis, thus generating an "umbrella" of optimal endpoints over the launch site. Each point on this

umbrella corresponded to a unique set of initial conditions. When an enemy trajectory was found to pierce the umbrella at a certain point, the correct firing angle and time for the interceptor could thus be found.

It was discovered that the optimum in the present case was very weak; arbitrary comparison trajectories gave nearly equal performance. This was thought to be due to the fact that the trajectory was extremely thrust-dominated, causing it to approximate a straight line.

VITA

Thomas W. Eagles

Candidate for the degree of

Master of Science

Thesis: OPTIMAL TRAJECTORIES FOR LOW ALTITUDE, HIGH ACCELERATION
ICBM INTERCEPTION

Major Field: Mechanical Engineering

Biographical:

> Personal Data: Born in Manhattan, Kansas, April 8, 1944, the son of
> Mrs. Helen Eagles and the late Gerry Patrick Eagles.

> Education: Attended Seven Dolors Grade School in Manhattan, Kansas;
> graduated from Luckey High School in 1962; attended Berkeley
> Summer Design Institute, summer, 1965; received the Bachelor
> of Science degree in Mechanical Engineering from Kansas State
> University in June, 1966.

> Professional experience: Worked as a student trainee-engineer under
> the NASA co-op program in the summer of 1963.